

BIOPHOTONICS

https://doi.org/10.1070/QEL16738

On the possibility of laser ektacytometry measurement of the kurtosis for erythrocyte deformability distribution

S.Yu. Nikitin

Abstract. **The problem of measuring red blood cell deformability by laser diffractometry in shear flow (ektacytometry) is considered. An algorithm has been developed for measuring the four central parameters of the erythrocyte deformability distribution, i.e. mean value, variance, asymmetry coefficient and kurtosis. The algorithm is designed to work with the peripheral part of the diffraction pattern and serves to analyse weakly inhomogeneous ensembles of red blood cells.**

Keywords: *red blood cell deformability, laser diffractometry, erythrocyte deformability distribution.*

1. Introduction

Deformability of red blood cells is one of the main rheological characteristics of blood [1, 2]. The task of measuring this parameter, taking into account the heterogeneity of red blood cell population, is very important [3], and possible approaches to its solution are discussed in [4–6]. In our work [7, 8], we have shown that laser ektacytometry makes it possible to measure the statistical characteristics of red blood cell ensembles: mean deformability, width and asymmetry of the erythrocyte deformability distribution. In this paper, we discuss the possibility of measuring another parameter – the coefficient of kurtosis for the distribution of red blood cells in terms of their deformability.

The coefficient of kurtosis is traditionally used to characterise the difference between the probability density distribution and the Gaussian distribution. One of the manifestations of this difference may be the bimodality of the structure of the erythrocyte deformability distribution, characteristic of some diseases, in particular for sickle cell anaemia and malaria. The measurement technique proposed by us can be useful in the diagnosis and treatment of these and other diseases associated with the impairment in blood cell deformability.

Laser ektacytometry is a method based on measuring the deformation of red blood cells under a given level of applied shear stress. The latter occurs during the flow of a suspension of erythrocytes through a thin capillary or a Couette-like system, when a fluid flow is produced in a gap between two plates as a result of the movement of one of them. Shear stress deforms (elongates) red blood cells and makes their shape close to ellipsoidal [3]. To visualise the shape of erythrocytes, the flow is illuminated by a laser beam and the resulting diffraction pattern is observed. Experience shows that with an increase in shear stress, the diffraction pattern is stretched in the direction perpendicular to the flow direction (Fig. 1a). The degree of diffraction pattern elongation serves as a measure of red blood cell deformability. The method of ektacytometry of red blood cells is described in more detail in [9–11].

S.Yu. Nikitin Faculty of Physics, M.V. Lomonosov Moscow State University, Vorob'evy gory, 119991 Moscow, Russia;
e-mail: sergeynikitin007@yandex.ru

Received 23 May 2018; revision received 6 September 2018
Kvantovaya Elektronika **48** (10) 983–987 (2018)
Translated by I.A. Ulitkin

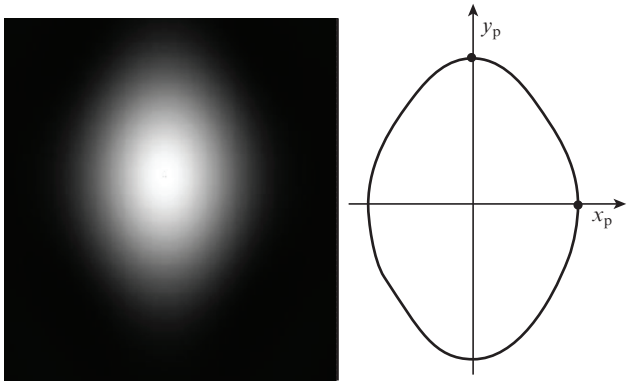

Figure 1. (a) Example of a diffraction pattern observed using a red blood cell ektacytometer and (b) isointensity curve and its polar points.

2. Red blood cell ensemble model

For a correct interpretation of the experimental data, a theory is needed that relates the characteristics of an ensemble of red blood cells with the parameters of the observed diffraction pattern. Following work [12, 13], an erythrocyte in shear flow will be modelled by a transparent elliptical disk. The semi-axes of the disk a and b are considered to be random variables and are defined by the formulae [14–17]

$$a = a_0(1 + \varepsilon), \quad b = b_0(1 - \varepsilon), \tag{1}$$

where a_0 and b_0 are the average dimensions of the semi-axes; and ε is a random parameter of the shape of particles with the following characteristics:

$$\langle\varepsilon\rangle = 0, \quad \mu = \langle\varepsilon^2\rangle, \quad \nu = \langle\varepsilon^3\rangle, \quad \delta = \langle\varepsilon^4\rangle. \tag{2}$$

In addition, we assume that

$$|\varepsilon| \ll 1, \tag{3}$$

that is, the heterogeneity of the ensemble in the particle shape is relatively weak. In this model, the mean red cell deformability is characterised by the parameter

$$s = a_0/b_0. \tag{4}$$

The red blood cell deformability distribution is described by the probability density $w(\varepsilon)$ for a random parameter ε. The parameters defined by formulae (2) represent the central parameters of this distribution. The coefficient of kurtosis is expressed through them by the formula

$$\mathrm{Ex} = \delta/\mu^2 - 3. \tag{5}$$

For a Gaussian random variable, Ex = 0.

3. Diffraction pattern characteristics

A diffraction pattern can be conveniently analysed using the concept of an isointensity curve, which is the curve on the observation screen with some constant value of the scattered light intensity. For healthy blood samples, shapes of isointensity curves are close to ellipses. For blood samples containing a fraction of weakly deformable cells (for example, in sickle cell anaemia), isointensity curves become rhombic [18].

To describe the shape of an isointensity curve, we use the Cartesian coordinate system on the observation screen. The origin of this system is placed at the centre of the diffraction pattern (the point of incidence of a direct laser beam), the x axis is directed horizontally, and the y axis is directed vertically. Physically, these directions differ in that one of them is parallel to the direction of the shear flow, and the other is perpendicular to it. In this coordinate system, the shape of the isointensity curve is described by the function $x = x(y)$ or $y = y(x)$. The points of intersection of the curve with the axes of coordinates are called the polar points of the isointensity curve (Fig. 1b). We denote the coordinate of the right polar point by x_p, and the top polar point – by y_p. The shape of the isointensity curve near the polar points is characterised by the derivatives of the functions $x(y)$ and $y(x)$, as well as by the dimensionless parameters

$$C_1 = \sqrt{x_\mathrm{p}\left|\frac{\mathrm{d}^2x}{\mathrm{d}y^2}(y=0)\right|}, \quad C_2 = \sqrt{y_\mathrm{p}\left|\frac{\mathrm{d}^2y}{\mathrm{d}x^2}(x=0)\right|},$$
$$C_3 = \sqrt[4]{\frac{1}{3}x_\mathrm{p}^3\left|\frac{\mathrm{d}^4x}{\mathrm{d}y^4}(y=0)\right|}, \quad C_4 = \sqrt[4]{\frac{1}{3}y_\mathrm{p}^3\left|\frac{\mathrm{d}^4y}{\mathrm{d}x^4}(x=0)\right|}. \tag{6}$$

In addition, the isointensity curve is characterised by the level of light intensity I or normalised intensity

$$f_0 = \frac{1}{4\beta^2}\frac{I}{I(0)}. \tag{7}$$

Here, $I(0)$ is the intensity of the central maximum of the diffraction pattern; and $\beta = -0.4$ is a constant value (a parameter of the Bessel function). To find the numbers C_1, C_2, C_3, and C_4, we need to choose the coefficients of the fourth-degree polynomials describing the shape of the isointensity curve near the polar points. These polynomials have the form:

$$y(x) = y_\mathrm{p} + \frac{1}{2}x^2\frac{\mathrm{d}^2y}{\mathrm{d}x^2}(x=0) + \frac{1}{4!}x^4\frac{\mathrm{d}^4y}{\mathrm{d}x^4}(x=0),$$

$$x(y) = x_\mathrm{p} + \frac{1}{2}y^2\frac{\mathrm{d}^2x}{\mathrm{d}y^2}(y=0) + \frac{1}{4!}y^4\frac{\mathrm{d}^4x}{\mathrm{d}y^4}(y=0).$$

We assume that the parameters f_0, C_1, C_2, C_3, and C_4 can be measured with a laser ektacytometer.

As an example, Fig. 2 shows the approximation of a circle by second- and fourth-degree polynomials. One can see that the fourth-degree polynomial significantly expands the region of similarity of the circle and its polynomial approximation. As applied to laser ektacytometry of red blood cells, this means that the approximation makes it possible to more fully reveal the features of the observed diffraction pattern and thus better to take into account the properties of the blood sample being investigated.

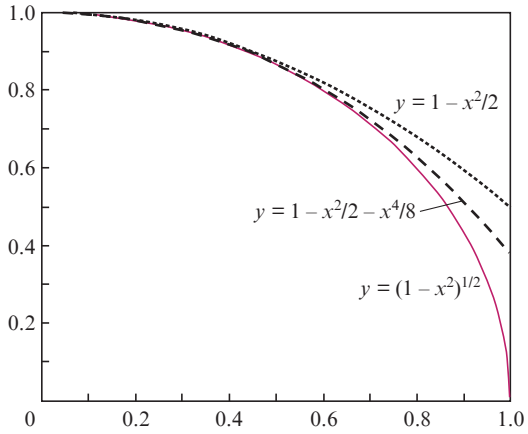

Figure 2. Approximation of a circle by second- and fourth-degree polynomials.

4. Diffractometric equations

In the model of flat elliptical disks, the distribution of light intensity on the observation screen is described by the formula [19]

$$I = I_0 N|\gamma|^2\left(a_0 b_0 \frac{k}{z}\right)^2\left\langle\left[(1-\varepsilon^2)\frac{J_1(q)}{q}\right]^2\right\rangle_\varepsilon, \tag{8}$$

where

$$q = \frac{k}{z}\sqrt{a_0^2x^2(1+\varepsilon)^2 + b_0^2y^2(1-\varepsilon)^2}; \tag{9}$$

I_0 is the intensity of the incident laser beam; N is the number of particles illuminated by the beam; z is the distance from the measuring volume to the observation screen; $k = 2\pi/\lambda$ is the wave number; λ is the wavelength of the light; and $J_1(x)$ is the first order Bessel function. The parameter $|\gamma|^2$ is determined by the thickness and optical density of the disk mimicking an erythrocyte; angle brackets denote averaging over an ensemble of red blood cells. Note that formulae (8) and (9) describe the distribution of the light intensity at those points of the observation screen where the direct laser beam is absent.

Assuming that $x = y = 0$, and also taking into account the asymptotics of the Bessel function and formulae (2), we find the intensity of light at the centre of the diffraction pattern:

$$I(0) = \frac{1}{4} I_0 N |\gamma|^2 \left(a_0 b_0 \frac{k}{z}\right)^2 (1 - 2\mu + \delta).$$

By normalising the intensity of light at an arbitrary point of the observation screen to the intensity of the central maximum, we obtain

$$\frac{I}{I(0)} = \frac{4}{1 - 2\mu + \delta} \left\langle \left[(1 - \varepsilon^2) \frac{J_1(q)}{q} \right]^2 \right\rangle_\varepsilon .$$

Laser ektacytometry traditionally makes use of the diffraction pattern region on the periphery of the central maximum, that is, near the first dark ring. This part of the diffraction pattern is most sensitive to the parameters of the ensemble of red blood cells [6]. The Bessel function in this region allows linear approximation:

$$J_1(q) = \beta(q - q_1).$$

Here $\beta = -0.4$ and $q_1 = 3.82$ are constant values (parameters of the Bessel function). In this case, the normalised distribution of light intensity takes the form:

$$\frac{I}{I(0)} = \frac{4\beta^2}{1 - 2\mu + \delta} \left\langle \left[(1 - \varepsilon^2) \left(1 - \frac{1}{p}\right) \right]^2 \right\rangle_\varepsilon , \tag{10}$$

where $p = q/q_1$.

We introduce the quantities $u = x/A$ and $v = y/B$, where

$$A = \frac{q_1 z}{k a_0}, \quad B = \frac{q_1 z}{k b_0} \tag{11}$$

are the parameters determining the size of the diffraction pattern, as well as $g = u^2 + v^2$ and $h = u^2 - v^2$. Then the expression for the parameter p takes the form

$$p = \sqrt{(1 + \varepsilon^2) g + 2\varepsilon h}\,.$$

Substituting this expression into formula (10), we obtain

$$\frac{I}{I(0)} = \frac{4\beta^2}{1 - 2\mu + \delta} f\,,$$

where $f = \langle \Phi \rangle_\varepsilon$; and

$$\Phi = \left[(1 - \varepsilon^2) \left(1 - \frac{1}{\sqrt{g(1 + \varepsilon^2) + 2h\varepsilon}} \right) \right]^2 .$$

We expand the function $\Phi(\varepsilon)$ into a Taylor series in powers of the parameter ε, and then average the resulting expression over an ensemble of erythrocytes. With formulae (2) taken into account, we obtain

$$\begin{aligned} gf = {} & (\sqrt{g} - 1)^2 + [(4 - 3\sqrt{g}) H^2 - 2g + 5\sqrt{g} - 3]\mu \\ & + [(-8 + 5\sqrt{g}) H^2 - 7\sqrt{g} + 8] \nu H + \frac{1}{4} [(64 - 35\sqrt{g}) H^4 \\ & + 2(-40 + 27\sqrt{g}) H^2 + 4g - 19\sqrt{g} + 16] \delta . \end{aligned} \tag{12}$$

Here, $H = h/g$. When $f = \text{const}$, this formula is an equation for the isointensity curve.

We introduce the polar coordinates r and φ, defining them by the formulae $u = r\cos\varphi$ and $v = r\sin\varphi$. Then, $g = r^2$, $h = r^2\cos(2\varphi)$, and

$$H = \cos(2\varphi). \tag{13}$$

In polar coordinates, the isointensity curve is described by the function $r = r(\varphi)$. The right polar point corresponds to $\varphi = 0$, and the upper polar point corresponds to $\varphi = \pi/2$. The equation for the function $r(\varphi)$ follows from equation (12) and has the form

$$\begin{aligned} & (1 - f_0)(1 - 2\mu + \delta) r^2 + \left[-2 + (-3H^2 + 5)\mu + (5H^2 - 7) \nu H \right. \\ & \left. + (-35H^4 + 54H^2 - 19) \frac{\delta}{4} \right] r + 1 + (4H^2 - 3)\mu \\ & + 8(-H^2 + 1) \nu H + 4(4H^4 - 5H^2 + 1)\delta = 0, \end{aligned}$$

or

$$\alpha r^2 - 2(1 + U) r + 1 + V = 0. \tag{14}$$

Here, f_0 is defined by formula (7);

$$\alpha = (1 - f_0)(1 - 2\mu + \delta); \tag{15}$$

$$U = \mu U_\mu + \nu U_\nu + \delta U_\delta; \quad V = \mu V_\mu + \nu V_\nu + \delta V_\delta; \tag{16}$$

$$\begin{aligned} & U_\mu = \frac{1}{2}(3H^2 - 5); \; U_\nu = \frac{1}{2}(7 - 5H^2) H\,; \\ & U_\delta = \frac{1}{8}(35H^4 - 54H^2 + 19); \end{aligned} \tag{17}$$

$$\begin{aligned} & V_\mu = 4H^2 - 3; \; V_\nu = 8(1 - H^2) H\,; \\ & V_\delta = 4(4H^4 - 5H^2 + 1) \end{aligned} \tag{18}$$

For a weakly inhomogeneous ensemble of erythrocytes, μ, ν , and δ are small parameters. In this case, an approximate solution of equation (14) can be represented as

$$r(\varphi) = \Gamma R(\varphi),$$

where

$$\Gamma = \frac{1}{(1 + \sqrt{f_0})(1 - 2\mu + \delta)},$$

and the function $R(\varphi)$ is described by the formula

$$R = 1 + \mu R_\mu + \nu R_\nu + \delta R_\delta + \mu^2 R_{\mu^2}. \tag{19}$$

Here,

$$R_\mu = \frac{1}{2\sqrt{f_0}} [-2U_\mu + (1 + \sqrt{f_0})(V_\mu - 2];$$

$$R_\nu = \frac{1}{2\sqrt{f_0}} [-2U_\nu + (1 + \sqrt{f_0}) V_\nu];$$

$$R_\delta = \frac{1}{2\sqrt{f_0}}[-2U_\delta + (1+\sqrt{f_0})V_\delta]; \tag{20}$$

$$R_{\mu^2} = \frac{1}{2\sqrt{f_0}}\left[-\frac{U_\mu^2}{1-\sqrt{f_0}} - (1+\sqrt{f_0})V_\mu\right].$$

Note that the function $R(\varphi)$ and its derivatives are linear in small parameters.

We introduce the functions

$$\tilde{u}(\varphi) = R(\varphi)\cos\varphi, \quad \tilde{v}(\varphi) = R(\varphi)\sin\varphi. \tag{21}$$

Then,

$$x(\varphi) = A\Gamma\tilde{u}(\varphi), \quad y(\varphi) = B\Gamma\tilde{v}(\varphi), \tag{22}$$

where $A\Gamma = \text{const}$ and $B\Gamma = \text{const}$. Using formulae (4), (6), (11), and (22), we obtain

$$C_1 s = \sqrt{\left|\tilde{u}\frac{\mathrm{d}^2\tilde{u}}{\mathrm{d}\tilde{v}^2}(0)\right|}, \quad C_3 s = \sqrt[4]{\frac{1}{3}\left|\tilde{u}^3\frac{\mathrm{d}^4\tilde{u}}{\mathrm{d}\tilde{v}^4}(0)\right|}, \tag{23}$$

$$\frac{C_2}{s} = \sqrt{\left|\tilde{v}\frac{\mathrm{d}^2\tilde{v}}{\mathrm{d}\tilde{u}^2}\left(\frac{\pi}{2}\right)\right|}, \quad \frac{C_4}{s} = \sqrt[4]{\frac{1}{3}\left|\tilde{v}^3\frac{\mathrm{d}^4\tilde{v}}{\mathrm{d}\tilde{u}^4}\left(\frac{\pi}{2}\right)\right|}. \tag{24}$$

Here, the functions $\tilde{u}(\varphi)$ and $\tilde{v}(\varphi)$ are defined by formulae (13), (17)–(21). Let us calculate the values of $C_1 s$ and $C_3 s$. Derivatives of $\mathrm{d}^2\tilde{u}/\mathrm{d}\tilde{v}^2$ and $\mathrm{d}^4\tilde{u}/\mathrm{d}\tilde{v}^4$ can be expressed in terms of derivatives of functions $\tilde{u}(\varphi)$ and $\tilde{v}(\varphi)$ with respect to the argument φ. Namely,

$$\frac{\mathrm{d}^2\tilde{u}}{\mathrm{d}\tilde{v}^2} = \frac{\tilde{u}''}{\tilde{v}'^2} - \frac{\tilde{u}'\tilde{v}''}{\tilde{v}'^3}, \tag{25}$$

$$\frac{\mathrm{d}^4\tilde{u}}{\mathrm{d}\tilde{v}^4} = \frac{\tilde{u}''''}{\tilde{v}'^4} - \frac{6\tilde{u}'''\tilde{v}'' + 4\tilde{u}''\tilde{v}''' + \tilde{u}'\tilde{v}''''}{\tilde{v}'^5} + 5\frac{(3\tilde{u}''\tilde{v}'' + 2\tilde{u}'\tilde{v}''')\tilde{v}''}{\tilde{v}'^6} - 15\frac{\tilde{u}'\tilde{v}''\tilde{v}''\tilde{v}''}{\tilde{v}'^7}. \tag{26}$$

The primes in these formulae denote the derivatives of the functions with respect to the argument φ.

Using formulae (13), (17)–(21), (23), (25), and (26), in the approximation of a weakly inhomogeneous ensemble of particles (3) we obtain

$$C_1 s = 1 + \mu q_1 - \nu q_2 + \delta q_3 - \mu^2 q_4, \tag{27}$$

$$C_3 s = 1 - \mu q_1 + \nu q_5 - \delta q_6 + \mu^2 q_7. \tag{28}$$

Here,

$$q_1 = 8 + \frac{2}{\sqrt{f_0}}; \quad q_2 = 16 + \frac{8}{\sqrt{f_0}}; \quad q_3 = 24 + \frac{16}{\sqrt{f_0}};$$

$$q_4 = \frac{2(1-4f_0)}{(1-\sqrt{f_0})\sqrt{f_0}}; \quad q_5 = 80 + \frac{28}{\sqrt{f_0}}; \tag{29}$$

$$q_6 = 280 + \frac{132}{\sqrt{f_0}}; \quad q_7 = \frac{38 - 8f_0}{(1-\sqrt{f_0})\sqrt{f_0}}.$$

Similarly, we calculate the values of C_2/s and C_4/s, defined by formulae (24):

$$\frac{C_2}{s} = 1 + \mu q_1 + \nu q_2 + \delta q_3 - \mu^2 q_4, \tag{30}$$

$$\frac{C_4}{s} = 1 - \mu q_1 - \nu q_5 - \delta q_6 + \mu^2 q_7. \tag{31}$$

Formulae (27), (28), (30), and (31) are diffractometric equations. They relate together the parameters of the diffraction pattern and the characteristics of the ensemble of red blood cells.

5. Algorithm of data processing

Equations (27), (28), (30), (31) can be rewritten in the form

$$\frac{C_2}{s} - C_1 s = 2\nu q_2, \tag{32}$$

$$C_3 s - \frac{C_4}{s} = 2\nu q_5, \tag{33}$$

$$D_1 = \mu q_1 + \delta q_3 - \mu^2 q_4, \tag{34}$$

$$D_2 = -\mu q_1 - \delta q_6 + \mu^2 q_7, \tag{35}$$

where

$$D_1 = \frac{1}{2}\left(C_1 s + \frac{C_2}{s}\right) - 1; \quad D_2 = \frac{1}{2}\left(C_3 s + \frac{C_4}{s}\right) - 1. \tag{36}$$

Having solved equations (32)–(35), we obtain

$$s = \sqrt{\frac{C_2 q_5 + C_4 q_2}{C_1 q_5 + C_3 q_2}}, \tag{37}$$

$$\mu = \frac{q_9}{q_8}\left(-1 + \sqrt{1 + D_3\frac{q_8}{q_9^2}}\right), \tag{38}$$

$$\nu = \frac{1}{2q_2}\left(\frac{C_2}{s} - C_1 s\right), \tag{39}$$

$$\delta = \frac{1}{q_8}(D_4 + \mu q_{10}). \tag{40}$$

Here,

$$q_8 = q_3 q_7 - q_4 q_6; \quad q_9 = \frac{1}{2}(q_6 - q_3)q_1; \quad q_{10} = (q_4 - q_7)q_1; \tag{41}$$

$$D_3 = D_1 q_6 + D_2 q_3; \text{ and } D_4 = D_1 q_7 + D_2 q_4 \tag{42}$$

Formulae (36)–(42) determine the algorithm for measuring the characteristics of erythrocyte deformability, whose input parameters are the numbers f_0, C_1, C_2, C_3, and C_4, defined by formulae (6), (7) and measured using a laser ektacytometer. The output parameters are the numbers s, μ, ν, and δ, defined by formulae (1), (2), and (4). These numbers characterise the red blood cell deformability distribution for a given blood sample. The sought values are found by successively applying formulae (29), (41), (37), (39), (36), (42), (38), (40), and (5).

6. Statistical moments of bimodal distribution

Consider bimodal erythrocyte ensemble deformability. For such an ensemble, the random parameter ε can take only two values, i.e. ε_1 and ε_2. Let p be the probability of the first of these values. Then, using notation (2), we can write:

$$p\varepsilon_1 + (1-p)\varepsilon_2 = 0, \quad p\varepsilon_1^2 + (1-p)\varepsilon_2^2 = \mu,$$

$$p\varepsilon_1^3 + (1-p)\varepsilon_2^3 = \nu, \quad p\varepsilon_1^4 + (1-p)\varepsilon_2^4 = \delta.$$

These formulae yield the equation

$$\delta - \mu^2 - \frac{\nu^2}{\mu} = 0.$$

Thus, for a bimodal random variable, there is a definite relationship between the central statistical moments of the second, third, and fourth orders. With regard to laser ektacytometry, this means that a certain combination of statistical moments, including the kurtosis of a distribution, can serve as an indicator of the modal structure of the red blood cell deformability distribution.

Thus, we have considered the problem of measuring the erythrocyte deformability by laser diffractometry (ektacytometry) in shear flow. An algorithm has been presented for measuring the four central parameters of the erythrocyte deformability distribution: mean value, dispersion, asymmetry coefficients and kurtosis. The algorithm is designed to work with the peripheral part of the diffraction pattern and serves to analyse weakly inhomogeneous ensembles of erythrocytes. The simultaneous determination of these parameters may be important for blood samples containing a fraction of weakly deformable cells (for example, in sickle cell anaemia).

Acknowledgements. The author is grateful to A.V. Priezzhev, V.D. Ustinov, E.G. Tsybrov, A.E. Lugovtsov and S. D. Shishkin for their help and useful discussions.

This work was supported by the Russian Foundation for Basic Research (Grant No. 17-02-00249).

References

1. Musielak M. *Clin. Hemorheol. Microcircul*., **42**, 47 (2009).
2. Kim Y., Kim K., Park Y., in *Blood Cell - An Overview of Studies in Hematology.* Ed. by E. Terry (Moschandreou, 2012) Chap. 10; DOI: 10.5772/50698 .
3. Dobbe J.G.G., Hardeman M.R., Streekstra G.J., Starckee J., Ince C., Grimbergen C.A. *Blood Cells, Molecules, and Diseases*, **28** (3), 373 (2002).
4. Plasek J., Marik T. *Appl. Opt*., **21**, 4335 (1982).
5. Rasia R.J., Schutz G. *Clin. Hemorheol*., **13**, 641 (1993).
6. Streekstra G.J., Dobbe J.G.G., Hoekstra A.G. *Opt. Express*, **18** (13), 14173 (2010).
7. Nikitin S.Yu., Lugovtsov A.E., Ustinov V.D., et al. *JIOHS*, **8**, 1550031 (2015); DOI: 10.1142/S1793545815500315.
8. Nikitin S.Yu., Ustinov V.D., Yurchuk Yu.S., et al. *JQSRT*, **178**, 315 (2016).
9. Bessis M., Mohandas N. *Blood Cells*, **1**, 307 (1975).
10. Hardeman M.R., Goedhart P.T., Dobbe J.G.G., Lettinga K.P. *Clin. Hemorheol*., **14** (4), 605 (1994).
11. Shin S., Ku Y., Park M.-S., Suh J.-S. *Cytometry Part B (Clin. Cytometry)*, **65B**, 6 (2005).
12. Nikitin S.Yu., Priezzhev A.V., Lugovtsov A.E., in *Advanced Optical Flow Cytometry: Methods and Disease Diagnoses.* Ed. by V.V. Tuchin (Wiley-VCH Verlag GmbH & Co., 2011) pp. 133–154.
13. Rabai M., Meiselman H.J., Wenby R.B., Detterich J.A., Feinberg J. *Biorheology*, **49**, 317 (2012); DOI: 10.3233/BIR-2012-0616.
14. Nikitin S.Yu., Kormacheva M.A., Priezzhev A.V., Lugovtsov A.E. *Quantum Electron*., **43** (1), 90 (2013) [*Kvantovaya Elektron*., **43** (1), 90 (2013)].
15. Nikitin S.Yu., Priezzhev A.V., Lugovtsov A.E., et al. *JQSRT*, **146**, 365 (2014).
16. Nikitin S.Yu., Ustinov V.D., Tsybrov E.G., Priezzhev A.V. *Izv. Saratov Univer., Novaya Ser. Ser. Fiz*., **17** (3), 150 (2017); DOI: 10.18500 / 1817-3020-2017-17-3-150-157; http://fizika.sgu.ru/ru/journal/issues.
17. Nikitin S.Yu., Ustinov V.D. *Quantum Electron*., **48** (1), 70 (2018) [*Kvantovaya Elektron*., **48** (1), 70 (2018)].
18. Renoux C., Parrow N., Faes C., et al. *Clin. Hemorheol. Microcirculat*., **62**, 173 (2016); DOI: 10.3233/CH-151979.
19. Nikitin S.Yu., Priezzhev A.V., Lugovtsov A.E. *JQSRT*, **8**, **121**, 1 (2013).